Irf3 Polymorphism Alters Induction of Interferon Beta in Response to *Listeria monocytogenes* Infection

Oleg Garifulin[1], Zanmei Qi[1], Haihong Shen[1,2,3¤], Sujatha Patnala[1], Michael R. Green[1,2,3], Victor Boyartchuk[1*]

1 Program in Gene Function and Expression, University of Massachusetts Medical School, Worcester, Massachusetts, United States of America, **2** Program in Molecular Medicine, University of Massachusetts Medical School, Worcester, Massachusetts, United States of America, **3** Howard Hughes Medical Institute, University of Massachusetts Medical School, Worcester, Massachusetts, United States of America

Genetic makeup of the host plays a significant role in the course and outcome of infection. Inbred strains of mice display a wide range of sensitivities to *Listeria monocytogenes* infection and thus serve as a good model for analysis of the effect of genetic polymorphism. The outcome of *L. monocytogenes* infection in mice is influenced by the ability of this bacterium to induce expression of interferon beta mRNA, encoded in mouse by the *Ifnb1* (interferon beta 1, fibroblast) gene. Mouse strains that lack components of the IFNβ signaling pathway are substantially more resistant to infection. We found that macrophages from the ByJ substrain of the common C57BL/6 inbred strain of mice are impaired in their ability to induce *Ifnb1* expression in response to bacterial and viral infections. We mapped the locus that controls differential expression of *Ifnb1* to a region on Chromosome 7 that includes interferon regulatory factor 3 *(Irf3),* which encodes a transcription factor responsible for early induction of *Ifnb1* expression. In C57BL/6ByJ mice, *Irf3* mRNA was inefficiently spliced, with a significant proportion of the transcripts retaining intron 5. Analysis of the *Irf3* locus identified a single base-pair polymorphism and revealed that intron 5 of *Irf3* is spliced by the atypical U12-type spliceosome. We found that the polymorphism disrupts a U12-type branchpoint and has a profound effect on the efficiency of splicing of *Irf3*. We demonstrate that a naturally occurring change in the splicing control element has a dramatic effect on the resistance to *L. monocytogenes* infection. Thus, the C57BL/6ByJ mouse strain serves as an example of how a mammalian host can counter bacterial virulence strategies by introducing subtle alteration of noncoding sequences.

Citation: Garifulin O, Qi Z, Shen H, Patnala S, Green MR, et al. (2007) *Irf3* polymorphism alters induction of interferon beta in response to *Listeria monocytogenes* infection. PLoS Genet 3(9): e152. doi:10.1371/journal.pgen.0030152

Introduction

Bacterial pathogens utilize a wide range of approaches to down-modulate or subvert host immune responses. *L. monocytogenes* is an intracellular pathogen that, following invasion of the host cell, is capable of escaping the host phagolysosomes and replicating in the cytoplasm. Within the cytoplasm, the bacterial DNA is thought to be recognized by an unknown host receptor, activating a signaling cascade that rapidly induces *Ifnb1* expression [1]. This signaling cascade relies on TANK-binding kinase 1 (TBK1)-mediated phosphorylation of IRF3, a transcription factor that, following dimerization and translocation to the nucleus, induces expression of *Ifnb1* [2–4].

In a murine model of infection, activation of host IFNβ signaling is an important *L. monocytogenes* virulence strategy. Mouse lines that lack components of the IFNβ signaling pathway (*Ifnb1, Ifnar1*) are significantly more resistant to *L. monocytogenes* infection [2,4–6]. A similar protective effect of a *Irf3* knockout suggests that Toll-like receptor (TLR)–independent induction of IFNβ is detrimental to control of listeriosis [7]. Several independent observations suggested that IFNβ signaling sensitizes lymphocytes for cell death, leading to an increase in sensitivity to *L. monocytogenes* [8]. *L. monocytogenes* activates such proapoptotic genes as *Trail (Tnfsf10), Pkr (Eif2ak2),* and *Daxx* in spleen and bone marrow macrophages of wild-type, but not *Ifnar*-deficient mice [4]. This is consistent with the observation that *Trail* knockout mice are more resistant to *L. monocytogenes* infection [9]. It has also been noted that following infection, mice lacking components of the IFNβ signaling machinery have higher total numbers of macrophages. This could be due to the ability of Type I interferon signaling to accelerate cell death of *L. monocytogenes*–infected macrophages [3].

Inbred mouse strains are extensively used as a model system to study host immune response throughout the course of *L. monocytogenes* infection. In addition, common strains display a wide range of sensitivities to intravenous infection with *L. monocytogenes* [10]. Our initial analysis of genetic determinants affecting susceptibility to *L. monocytogenes*

Editor: Derry C. Roopenian, The Jackson Laboratory, United States of America

Received May 14, 2007; **Accepted** July 19, 2007; **Published** September 7, 2007

A previous version of this article appeared as an Early Online Release on July 20, 2007 (doi:10.1371/journal.pgen.0030152.eor).

Copyright: © 2007 Garifulin et al. This is an open-access article distributed under the terms of the Creative Commons Attribution License, which permits unrestricted use, distribution, and reproduction in any medium, provided the original author and source are credited.

Abbreviations: BMM, bone marrow macrophage; cfu, colony-forming units; HU, hemagglutinizing unit; LDH, lactose dehydrogenase; MOI, multiplicity of infection; RI, recombinant inbred; RT-PCR, reverse transcriptase PCR; TLR, Toll-like receptor

* To whom correspondence should be addressed. E-mail: victor.boyartchuk@umassmed.edu

¤ Current address: Department of Life Science, Gwangju Insitute of Science and Technology, Oryong-dong, Republic of Korea

Author Summary

Specific variances in an individual's DNA, known as genetic polymorphisms, can play a significant role in determining susceptibility to an infectious disease. To identify the genetic polymorphisms that are associated with resistance to the common human bacterial pathogen *L. monocytogenes,* we have carried out a series of genetic and molecular biology experiments using closely related strains of mice that are differentially susceptible to *Listeria* infection. Through this analysis, we have identified a spontaneous mutation in an intron of the *Irf3* gene, which encodes a key transcription factor involved in innate immunity. This single nucleotide change affects the efficiency with which *Irf3* mRNA is spliced, thus limiting the ability of bacteria to induce interferon beta expression in order to suppress innate immune defense. By analyzing this mutation, we found that processing of mouse *Irf3* mRNA relies on an atypical U12 splicing mechanism that has been suggested to be a rate-limiting step in gene expression. Our findings not only provide an additional example of an important role of noncoding polymorphisms in control of gene function, but also demonstrate how such polymorphisms can fine tune innate immune response.

infection was carried out using a pair of differentially susceptible inbred mouse strains: BALB/cByJ and C57BL/6ByJ [11]. These strains were selected based on the ancestry of the 13-member CXB Recombinant Inbred (RI) Panel, which serves as a useful tool for mapping single gene traits [12]. While our study identified two major genetic loci that controlled differential sensitivity to *L. monocytogenes* infection, it was clear that there were additional genetic factors that we did not detect due to the limited size of our cross. Here, we report identification and characterization of one of these additional factors, a polymorphism in the C57BL/6ByJ inbred mouse strain that affects expression of *Ifnb1* and results in increased resistance to *L. monocytogenes* infection. Our data demonstrate that a single base-pair polymorphism in intron 5 of *Irf3* reveals an important role for splicing in control of IFNβ induction and innate immune function.

Results

C57BL/6ByJ Strain-Specific Defect in Induction of *Ifnb1* Expression

Our analysis of *L. monocytogenes* infection of macrophages derived from bone marrow (i.e., bone marrow macrophages; BMMs) of BALB/cByJ and C57BL/6ByJ strains revealed strain-specific differences in infection-induced cell death. Across a range of time points and infectious doses, BALB/cByJ BMMs had consistently higher cell death then BMMs from C57BL/6ByJ mice (Figure 1A and 1B). Interestingly, 18 h following infection with *L. monocytogenes*, there were also significant ($p < 0.001$) differences in death of BMMs from J and ByJ substrains of the common C57BL/6 lineage (Figure 1C). The observed differences in cell death could be due to small differences in replication of bacteria in infected BMMs (Figure 1D). However, recent studies that have demonstrated a role for IFNβ signaling in the outcome of *L. monocytogenes* infection have also suggested that it plays a role in the survival of macrophages [2]. Therefore, we chose to test if there are mouse strain-specific differences in IFNβ signaling, and we analyzed the course of *Ifnb1* mRNA induction in *L. monocytogenes*–infected BMMs. We found that *Ifnb1* expression was rapidly induced in BALB/cByJ BMMs, increasing 400-fold by the 4-h time point. By contrast, in C57BL/6ByJ BMMs, there was very slight induction of *Ifnb1* mRNA, reaching only 12-fold by the 4-h time point (Figure 2A). This low level of *Ifnb1* induction in C57BL/6ByJ mice was surprising, as the role of *Ifnb1* signaling in conferring susceptibility to *L. monocytogenes* infection has been analyzed using mice of the C57BL/6 background [4]. To test the possibility that the defect in *Ifnb1* induction was specific to the C57BL/6ByJ substrain we also monitored expression of *Ifnb1* in BMMs from C57BL/6J mice. Indeed, in response to *L. monocytogenes* infection, C57BL/6J BMMs had a similar magnitude of *Ifnb1* mRNA induction as BALB/cByJ BMMs (Figure 2A). *Ifnb1* mRNA induction in F1 progeny of the J and ByJ substrains of mice was similar to that observed in the C57BL/6J strains (unpublished data), suggesting that the C57BL/6ByJ strain carries a recessive polymorphism that prevents upregulation of *Ifnb1* expression. There is at least one additional inbred mouse strain, SPRET/Ei, that has a similar naturally occurring defect in induction of *Ifnb1* expression [13]. However, the genetic basis for this defect in SPRET/Ei remains to be elucidated.

Differential Sensitivity of C57BL/6 Substrains to *L. monocytogenes* Infection

Several lines of evidence indicate that inhibition of IFNβ signaling in mice leads to a significant increase in resistance to intravenous *L. monocytogenes* infection [4,5]. To test if the *Ifnb1* induction defect in the C57BL/6ByJ strain promotes resistance to infection, we compared survival and bacterial loads in C57BL/6 substrains infected intravenously with a high dose (10^5 colony-forming units [cfu]) of *L. monocytogenes* strain 10403S. There was no detectable *Ifnb1* expressed in liver and spleen tissue in either mouse strain up until the 24-h time point. At the 24-h time point, *Ifnb1* mRNA was present in both livers and spleens of C57BL/6J animals but only in spleens of C57BL/6ByJ animals (Figure S1). We found that at the 24- and 48-h time points, there was a significantly higher number of bacteria in the livers (Figure 3A) and spleens (Figure 3B) of C57BL/6J mice, indicating the infection was controlled better in C57BL/6ByJ mice. Consistent with this idea, spleens from C57BL/6ByJ animals had nearly twice as many Mac1-positive cells than spleens from C57BL/6J mice at the 48-h time point (Figure 3C). In fact, this dose of bacteria led to death in C57BL/6J animals within 72 h after infection, whereas most of the C57BL6/ByJ mice survived indefinitely (Figure S2). Collectively, these results indicate that C57BL/6ByJ mice were significantly more resistant to intravenous *L. monocytogenes* infection than C57BL/6J animals.

Ifnb1 Induction Defect Lies in a Shared Component of the Signaling Pathway

Intracellular *L. monocytogenes* is thought to induce *Ifnb1* expression by activating an as-of-yet unidentified cytoplasmic receptor that initiates signaling through the TBK1 and inhibitor of kappaB kinase epsilon (IKBKE) kinases [1]. TBK1 and IKBKE also participate in transducing signals from various TLRs in response to viral and bacterial infections [14]. Therefore, we tested if the defect in C57BL/6ByJ mice was in a *L. monocytogenes*–specific component of the TBK1/IKBKE signaling pathway or in a component shared with other pathways. Treatment of C57BL/6ByJ BMMs with

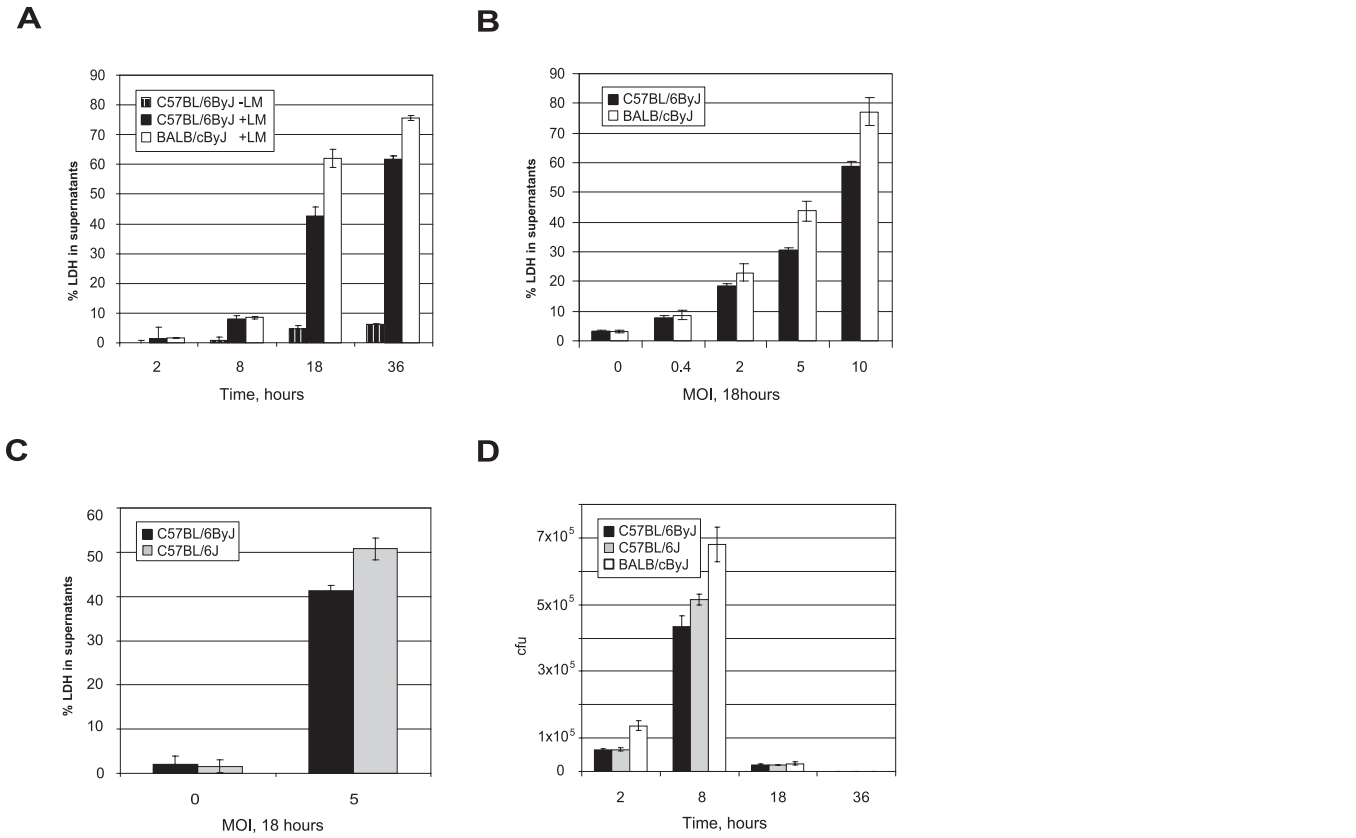

Figure 1. Induction of Macrophage Cell Death by Infection with *L. monocytogenes*

(A) Mice were infected with *L. monocytogenes* (LM) at MOI5 and BMM cell death was monitored by the release of the cytosolic enzyme LDH into the supernatant. Over the 36-h time period a greater proportion of BALB/cByJ BMMs than of C57BL/6ByJ BMMs died as a result of infection.
(B) Differences in death of C57BL6/ByJ and BALB/cByJ macrophages were maintained across varying MOIs at 18 h post infection.
(C) BMMs from C57BL/6 substrains infected for 18 h with *L. monocytogenes* at MOI5 had significantly different amounts of dead cells ($p < 0.001$).
(D) Death of BMMs exposed intracellular *L. monocytogenes* to gentamicin in the media, resulting in reduction of recovered bacteria after the 8-h time point.
doi:10.1371/journal.pgen.0030152.g001

lipopolysaccharide or poly I:poly C, which induce *Ifnb1* expression through TLR4 and TLR3, respectively, failed to induce *Ifnb1* mRNA at the same levels as observed in C57BL/6J BMMs (Figure 2B and 2C). On the other hand, C57BL/6ByJ BMMs treated with 200 hemagglutinizing units (HU) of Sendai virus, which induces *Ifnb1* expression through a RIG-I/MAVS–dependent pathway [15], had levels of *Ifnb1* mRNA comparable to those observed in C57BL/6J BMMs at the later stages of infection but nevertheless had a noticeable delay at the earlier stages (Figure 2D). These observations indicate that the defect in *Ifnb1* induction in C57BL/6ByJ mice is likely to lie in a shared component of the signaling pathway. However, our initial analysis *Tbk1, Ikbke,* and *Irf3* failed to identify differences in the coding sequence or overall expression levels of these mRNAs in C57BL/6ByJ versus C57BL/6J mice (unpublished data).

Mapping of the *Ifnb1* Induction Trait

As mentioned above, our original choice of mouse strain for genetic analysis was based on the availability of the CXB RI mapping panel. However, analysis of the transcriptional response to *L. monocytogenes* infection in macrophages from all 13 CXB strains revealed no differences in induction of *Ifnb1* (unpublished data), precluding the use of the panel for mapping. Because C57BL/6ByJ mice carry a recessive mutation, we therefore chose a backcross as our mapping strategy to identify the locus in the C57BL/6ByJ mouse genome that harbors the mutation preventing induction of *Ifnb1*. C57BL/ByJ and C57BL/6J mice have virtually no polymorphisms that can be used to monitor allelic segregation in a cross. On the other hand, BALB/cByJ mice are similar to C57BL/6J mice in their induction of *Ifnb1,* and we therefore chose C57BL/6ByJ and BALB/cByJ as parental strains for our cross. We backcrossed F1 male progeny of C57BL/6ByJ and BALB/cByJ mice to C57BL/6ByJ females and used the resulting 54 C(B.C) N2 progeny to construct a genetic map with 56 microsatellite markers evenly distributed throughout the mouse genome [16]. To generate phenotypic data, we first used real time reverse transcriptase PCR (RT-PCR) to analyze the dynamics of *L. monocytogenes*-induced *Ifnb1* expression in BMMs isolated from 43 backcrossed mice (unpublished data). We then used transformed real time RT-PCR Ct values representing the levels of *Ifnb1* mRNA at the 4-h time point directly as a quantitative trait. Mapping of this trait using MapManger QTX identified a peak likelihood ratio statistic score of 35.1 (logarithm of the odds [LOD] = 7.6) at the D7Mit229 marker [17] (Figure S3). Using the MapManger QTX built-in permutation test function, we established that the identified linkage is highly significant with an experimental *p*-value less

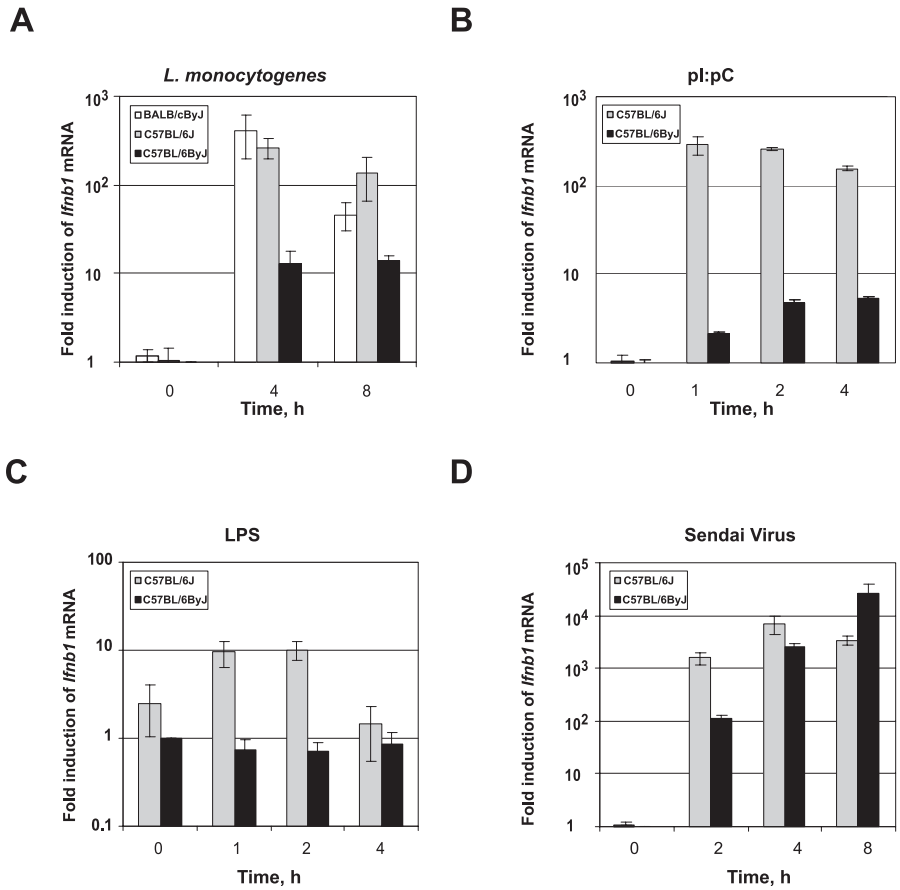

Figure 2. Mouse Strain-Specific Differences in Induction of *Ifnb1* mRNA Measured by Real Time RT-PCR

(A) In response to *L. monocytogenes* infection, C57BL/6ByJ BMMs show nearly 100-fold lower induction of Ifnb1 mRNA compared to BMMs from BALB/cByJ and C57BL/6J strains.

(B, C) Treatment of BMMs with 25 μg/ml poly I:poly C (B) or 1 μg/ml lipopolysaccharide (C) fails to appreciably induce *Ifnb1* mRNA in C57BL/6ByJ mice.

(D) Incubation of BMM with 200 HU of Sendai Virus demonstrates delayed kinetics of *Ifnb1* induction in C57BL/6ByJ mice. All figures are representatives of at least three independent experiments (±STD, n=4). *Ifnb1* mRNA induction is measured relative to the uninduced *Ifnb1* mRNA levels in C57BL/6J BMMs.

doi:10.1371/journal.pgen.0030152.g002

then 10^{-4}. QTL support interval was approximated as 1.5 LOD drop-off from the peak score [18] and extended from D7Mit27 to D7Mit158 markers, spanning empirical genetic distance of 6.9 cM (0 cM MGI) and a physical fragment of 2.35 Mb. The D7Mit229 marker is located on mouse Chromosome 7 adjacent to *Irf3* [16], identifying *Irf3* as the primary candidate gene.

Irf3 mRNA in C57BL/6ByJ Strain Is Not Efficiently Spliced

Interestingly, our initial analysis of C57BL/6J and C57BL/6ByJ substrains did not find any differences in overall *Irf3* mRNA levels or polymorphisms in the coding region of *Irf3* (unpublished data). However, analysis of the structure of *Irf3* mRNA using a series of overlapping primers revealed differences in the *Irf3* transcripts between the two substrains. As expected, in C57BL/6J mice the majority of *Irf3* transcripts were completely spliced, whereas in C57BL/6ByJ mice, splicing of *Irf3* was not complete and the majority of transcripts retained intron 5 (Figure 4A and quantified in Figure 4B). Retention of intron 5 introduces a premature stop codon at amino acid 243, rather than producing the full-length 419 amino-acid protein. To test if the observed differences in splicing had functional significance, we analyzed activation of IRF3 in BMMs by monitoring the formation of IRF3 dimers following bacterial *(L. monocytogenes)* or viral (Sendai virus) infection. We found that untreated BMMs from C57BL/6ByJ mice had significantly lower levels of IRF3 protein than untreated BMMs from C57BL/6J mice (Figure 4C and 4D). Moreover, following a 2-h infection with *L. monocytogenes* or Sendai virus, there were no detectable IRF3 dimers in C57BL/6ByJ BMMs, although IRF3 dimers were readily detectable in C57BL/6J BMMs. Nevertheless, we observed that Sendai virus–infected C57BL/6ByJ BMMs are capable of inducing *Ifnb1* expression (see Figure 2D). This is consistent with earlier observations that *Irf3*-deficient cells rely on IRF7 to have a normal interferon response to several viral infections [19,20]. Interestingly, our polyclonal antibodies failed to detect a truncated form of IRF3 even in the presence of proteasome inhibitor (MG132), suggesting that the unspliced form of *Irf3* might not be efficiently translated (Figure 4C). Overall, these results show that C57BL/6ByJ BMMs have dramatically lower amounts of functional IRF3 protein, and in conjunction with the existing *Irf3* knock-out data [2,4], explain the increased resistance of C57BL/6ByJ mice to *L. monocytogenes* infection (see Figure 3).

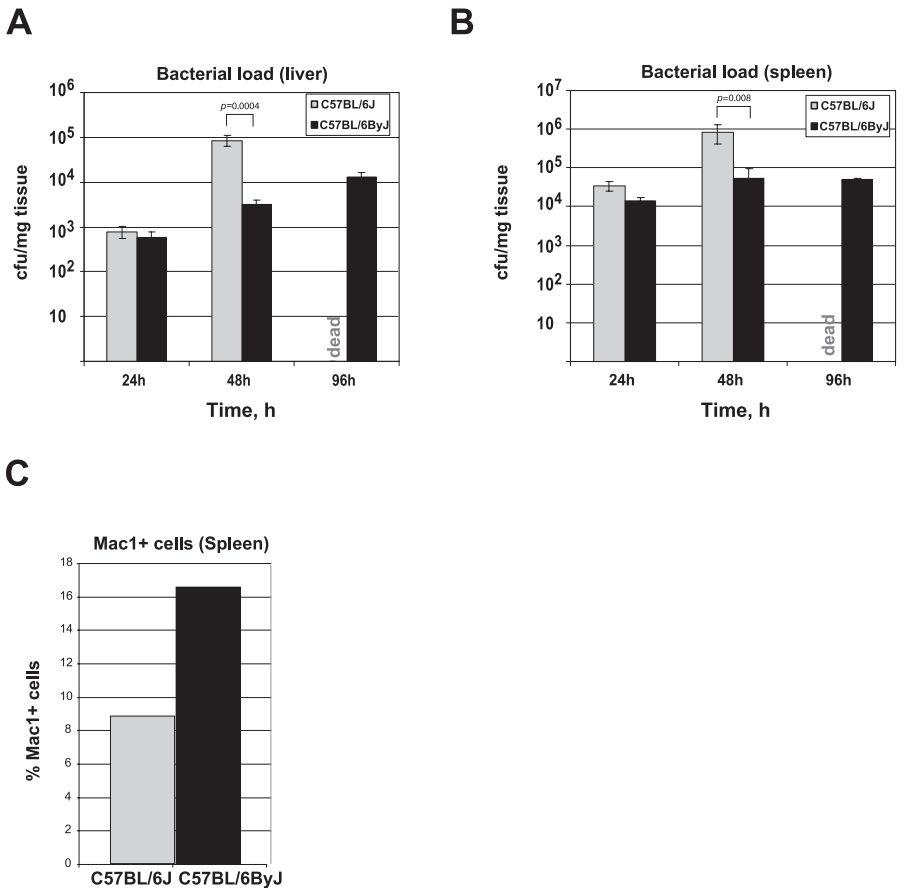

Figure 3. Differences in Susceptibility to *L. monocytogenes* Infection of C57BL/6 Substrains

(A, B) C57BL/6J mice have significantly elevated bacterial loads in their livers (A) and spleens (B) at all time points following intravenous infection with 10^5 cfu *L. monocytogenes*. At the 96-h time point following infection all C57BL/6J mice were dead.

(C) C57BL/6ByJ mice have twice as many Mac-1 positive cells in their spleens than C57BL/6J mice at the 48-h time point post infection.

doi:10.1371/journal.pgen.0030152.g003

A to T Polymorphism Impairs Slicing of *Irf3* Intron 5 in C57BL/6ByJ Strain

Sequencing of the entire 7.2-kb genomic region of *Irf3* [21], including 1 kb of upstream and downstream sequences, revealed a single A to T polymorphism in the middle of intron 5 in C57BL/6ByJ mice (Figure 5). To establish if this polymorphism altered the splicing efficiency of the intron, we monitored splicing using both cell culture–based and in vitro approaches. For cell culture–based experiments, we derived minigene constructs containing the complete intron 5 (from either C57BL/6J or C57Bl/6ByJ) flanked by exons 5 and 6, and expressed them under the control of the heterologous CMV promoter. In order to rule out the possibility that C57BL/6ByJ mice carry additional mutations that affect splicing, we first tested our constructs in a C57BL/6ByJ fibroblast-like cell line (Y5). Following transfection into Y5 cells, the efficiency of splicing of intron 5 was monitored by real time RT-PCR using primers specific to the vector and exon 5–6 junctions, and the total amount of RNA expressed from each construct was measured using primers specific to the exon fragment, which is identical in both constructs (see Figure 6A schematic). When normalized for the total amount of expressed RNA, there was significantly more spliced product generated from the C57BL/6J construct than from the C57BL/6ByJ construct (Figure 6A). This result indicates that in C57BL/6ByJ cells, C57BL/6J *Irf3* intron 5 is spliced more efficiently than the C57BL/6ByJ version of the intron.

The effect of the A to T substitution on splicing efficiency of intron 5 was further confirmed using an in vitro splicing assay, in which a uniformly radioactively labeled *Irf3* pre-mRNA containing intron 5 flanked by 50 bp of exon 5 and exon 6 was incubated in HeLa nuclear extract. As expected, the C57BL/6J-derived *Irf3* pre-mRNA substrate was spliced efficiently, as evidenced by the appearance of both intermediate and fully spliced products (Figure 6B). By contrast, there was no detectable splicing of the C57BL/6ByJ-derived *Irf3* pre-mRNA substrate even when incubated for 60 min in the splicing reaction mixture. These results confirmed that the A to T substitution had a direct effect on efficiency of *Irf3* splicing.

Splicing of Murine *Irf3* Intron 5 Relies on U12 Splicesome

Pre-mRNA splicing occurs in a ribonucleoprotein complex called the spliceosome [22]. Splicing is initiated through recognition of several intron-defining splicing signals, including the 5′ and 3′ splice sites and the branchpoint, which is usually located near the 3′ end of the intron. Introns can be classified into two categories: U2-type introns, which comprise the major class of introns, and U12-type introns. U2-type introns are characterized by the presence of a conserved

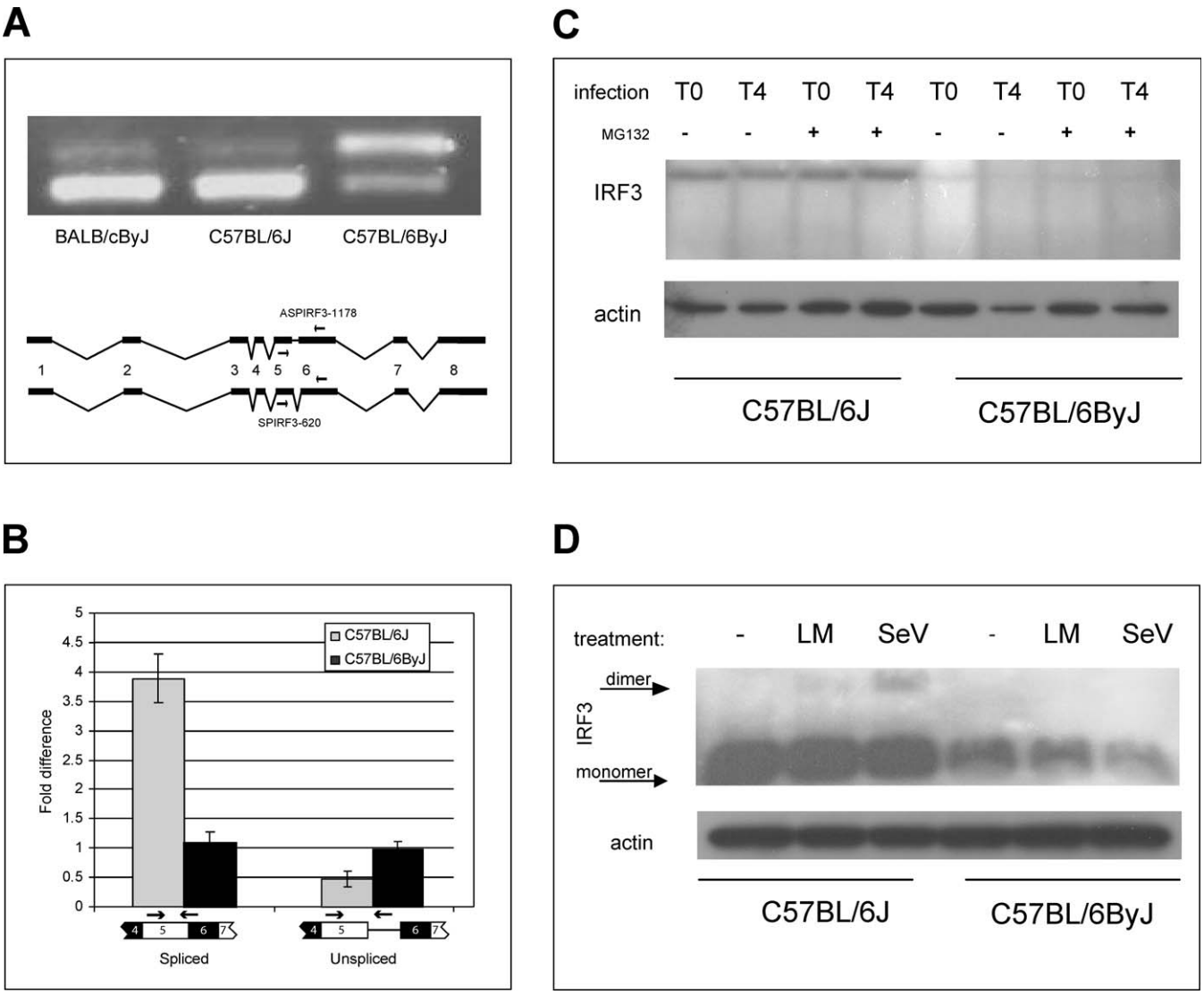

Figure 4. Mouse Strain-Specific Differences in *Irf3* mRNA and Protein Levels

(A) The majority of C57BL/6ByJ BMM *Irf3* transcripts retain intron 5 (upper band), whereas in both C57BL/6J and BALB/cByJ strains most of *Irf3* pre-mRNA is properly spliced.

(B) In C57BL/6J BMMs, there is on average 4-fold more ($p < 0.0001$) fully spliced and 2-fold less ($p < 0.01$) unspliced *Irf3* transcripts than in C57BL/6ByJ BMMs. Amounts of *Irf3* mRNA were measured relative to a C57BL/6ByJ sample using primer pairs specific to denoted areas of the *Irf3* mRNA (±STD, $n = 6$).

(C) Inefficient splicing of *Irf3* results in decreased levels of IRF3 protein in unstimulated (T0) and *L. monocytogenes*-infected (T4) C57BL/6ByJ macrophages. The truncated version of IRF3 predicted to be produced by translation of unspliced *Irf3* mRNA was not detected even in the presence of the proteosomal inhibitor MG132.

(D) Two-hour infection of C57BL/6J BMMs with either *L. monocytogenes* (LM) or Sendai Virus (SeV) leads to formation of the transcriptionally active IRF3 dimer, whereas infection of C57BL/6ByJ cells produces virtually undetectable amounts of IRF3 dimer. Total amount of loaded protein was monitored by immunoblotting with an anti-actin antibody.

doi:10.1371/journal.pgen.0030152.g004

GU dinucleotide at the 5′ end of the intron and a conserved AG dinucleotide at the 3′ end, whereas U12-type introns can harbor AT–AC, AT–AG, and GU–AG dinucleotides at their 5′ and 3′ boundaries, respectively. Furthermore, on U12-type introns, the 5′ and 3′ splice sites and branchpoint are highly conserved and differ from those of the conventional U2-type introns [23,24], and the characteristic polypyrimidine tract is typically absent [25].

Because the A to T polymorphism is located within an intron and affects splicing efficiency, we hypothesized that it might alter the function of a splicing signal. The polymorphism is located 46 bp upstream of the 3′ splice site, within a region where the branchpoint is typically found. The 5′ boundary of the murine *Irf3* intron 5 matches the U2-type intron GTRAGT consensus sequence (Figure 5) [23,24]. However, the region surrounding the polymorphism more closely resembled the U12 branchpoint consensus (TCCTTA-ACY) than the U2 branchpoint consensus (YURAY). To determine whether intron 5 of the *Irf3* gene was a U2-type or U12-type intron, we monitored splicing of the wild-type C57BL/6J-derived *Irf3* pre-mRNA substrate following inactivation of U2 or U12 snRNA by oligonucleotide-directed

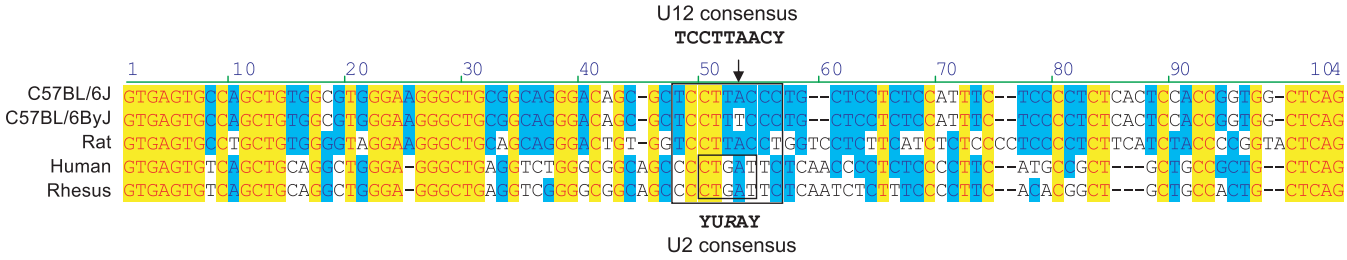

Figure 5. Alignment of the Intron 5 Sequences from the *Irf3* Genes from Mouse (Substrains C57BL/6J and C57BL/6ByJ), Rat, Human, and Rhesus Monkey
The A to T polymorphism (arrow) observed in the *Irf3* gene in C57BL/6ByJ mice is found within a conserved sequence (boxed) similar to the U12 TCCTAACY branchpoint consensus. A T to G substitution found in the human and rhesus genes converts a pyrimidine to a purine residue in front of a putative branchpoint adenosine and creates a perfect match (inset box) to the U2 YURAY branchpoint consensus.
doi:10.1371/journal.pgen.0030152.g005

RNase H cleavage. The in vitro splicing assay in Figure 6C shows that splicing of the C57BL/6J-derived *Irf3* pre-mRNA substrate occurred following inactivation of U2 snRNA but not following inactivation of U12 snRNA. As expected, splicing of the control U2-type intron–containing adenovirus major late (Ad ML) pre-mRNA substrate was fully dependent on the presence of U2 snRNA. These observations indicate that splicing of intron 5 of the *Irf3* gene relies on the U12-dependent mechanism.

Irf3 Intron 5 A to T Polymorphism Affects Induction of *Ifnb1* Expression

Irf3 transcripts that retain intron 5 are detected in both C57BL/6ByJ and C57BL/6J strains (see Figure 4A). Therefore, it appears that even in the C57BL/6J strain splicing of intron 5 is somewhat inefficient, whereas in the C57BL/6ByJ strain, intron 5 splicing is substantially impaired. To test if the observed phenotypic differences in induction of *Ifnb1* expression in the two mouse strains are due to differences in splicing efficiency of *Irf3* intron 5, we performed complementation experiments. To achieve this, we transfected BMMs from *Irf3* knockout mice with full-length in vitro transcribed *Irf3* mRNA species harboring either the C57BL/6J or C57BL/6ByJ version of intron 5. Fully spliced *Irf3* mRNA was used as a positive control, and mRNA containing a partial deletion of IRF domain (ΔXma) was used as a negative control. Previous experiments had shown that introduction of single-stranded RNA into the cell cytosol leads to *Irf3*-dependent induction of *Ifnb1* expression [26–28] (O. G., unpublished data). Therefore, transfection of intron 5–containing *Irf3* mRNAs into BMMs that lack *Irf3* should lead to a level of *Ifnb1* induction that is proportional to the splicing efficiency of intron 5. We measured the levels of *Ifnb1* mRNA by real time RT-PCR 19 h following transfection of BMMs, and found that there was ~5-fold more ($p < 0.01$) *Ifnb1* mRNA expressed in BMMs transfected with the C57BL/6J-derived *Irf3* mRNA than in BMMs transfected with C57BL/6ByJ-derived *Irf3* mRNA (Figure 7). Following a 4-h infection with *L. monocytogenes,* BMMs transfected with either mRNA showed further induction of *Ifnb1* expression. Nevertheless, the C57BL/6J-derived *Irf3* mRNA induced significantly ($p < 0.01$) higher amounts of *Ifnb1* mRNA than the C57BL/6ByJ-derived version. As expected, BMMs transfected with *Irf3* mRNA lacking the IRF domain induced only low levels of *Ifnb1* mRNA expression. Because the *Irf3* knockout mice used in this experiment are on the C57BL/6J background [19], this experiment also ruled out the possibility that impaired splicing of *Irf3* intron 5 could be due to a linked C57BL/6ByJ polymorphism. Therefore, we conclude that decreased splicing efficiency of *Irf3* intron 5 is directly responsible for the reduction in *Ifnb1* expression observed in C57BL/6ByJ mice.

Discussion

Previous studies have demonstrated an important role of IFNβ signaling in host defense against *L. monocytogenes* infection. *L. monocytogenes* evolved to take advantage of the host signaling pathways and is capable of inducing *Ifnb1* expression in order to down-modulate the antibacterial host defense. Here, we show that at least one inbred strain of mice can resist this pathogen's tactic by carrying a single nucleotide polymorphism that changes the efficiency of splicing of its *Irf3* transcription factor. While this naturally occurring polymorphism does not eliminate IRF3 activity, the resulting reduction in IRF3 protein levels is sufficient to confer 10-fold higher resistance to *L. monocytogenes* infection. Considering that complete loss of IRF3 function is detrimental to immune defense, and *Irf3* knockout mice are more sensitive to encephalomyocarditis infection [19], it would be interesting to determine if the level of IRF3 in C57BL/6ByJ mice is sufficient to maintain protection against viral infections. Nevertheless, our finding indicates that genetic changes in noncoding regions of the host genome is one of the mechanisms that can be used to fine tune the effectiveness of host defenses against infections.

It has been suggested that in the process of evolution, U12-type introns are either lost or undergo subtype switching (from AT–AC to GT–AG) and are eventually converted to U2-type introns [25]. Our data provide additional support for this hypothesis. Although splicing of *IRF3* intron 5 is dependent on the U12 spliceosome, the splice donor site is a typical U2 site. Even more interesting is the fact that the region of the human and rhesus intron 5 that is homologous to the putative murine U12 branchpoint site contains a G in place of the T that is found in rodents (Figure 5, inset box). This substitution places a purine residue in front of a putative branchpoint adenosine, thus creating a perfect match to the canonical U2 branchpoint consensus sequence. Therefore, intron 5 of the murine *Irf3* gene might represent one of the final steps in the conversion of a U12-type intron to a U2-type intron.

The amount of IRF3 available in the cell is tightly controlled and overproduction of IRF3 is lethal to BMMs

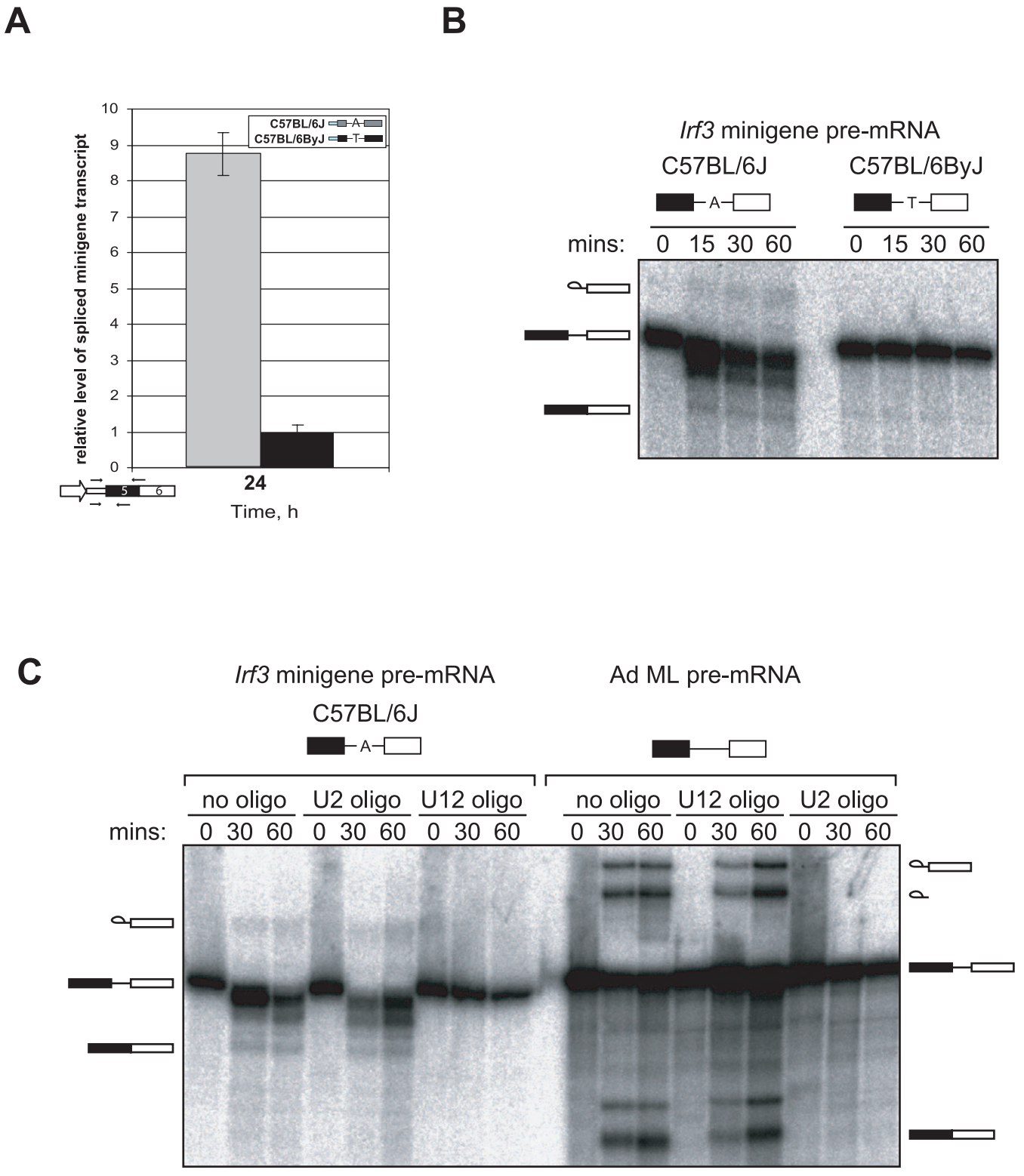

Figure 6. Mouse Strain-Specific Differences in *Irf3* Intron 5 Splicing

(A) Relative levels of the spliced to unspliced forms of an *Irf3* intron 5–containing minigene expressed in C57BL/6ByJ fibroblast-like Y5 cells 12 h following transfection. Levels are normalized to the total amount of expressed RNA. The location of the primers used in the analysis is shown in the schematic diagram. The efficiency of splicing of intron 5 was monitored using primers specific to the vector and exon 5–6 junctions (top pair), whereas the total amount of RNA expressed from each construct was measured using primers specific to the exon fragment (bottom pair).

(B) In vitro splicing of the C57BL/6J of C57BL/6ByJ minigene pre-mRNA was analyzed at 0, 15, 30, and 60 min following addition of the substrate to the nuclear extract. Identities of the spliced products are shown of the left.

(C) In vitro splicing of the C57BL/6J minigene pre-mRNA was analyzed at 0, 30, and 60 min following inactivation of U2 or U12 snRNA by oligonucleotide directed RNase H cleavage. As a control, splicing of the U2-type intron–containing adenovirus major late (Ad ML) pre-mRNA substrate was analyzed.

doi:10.1371/journal.pgen.0030152.g006

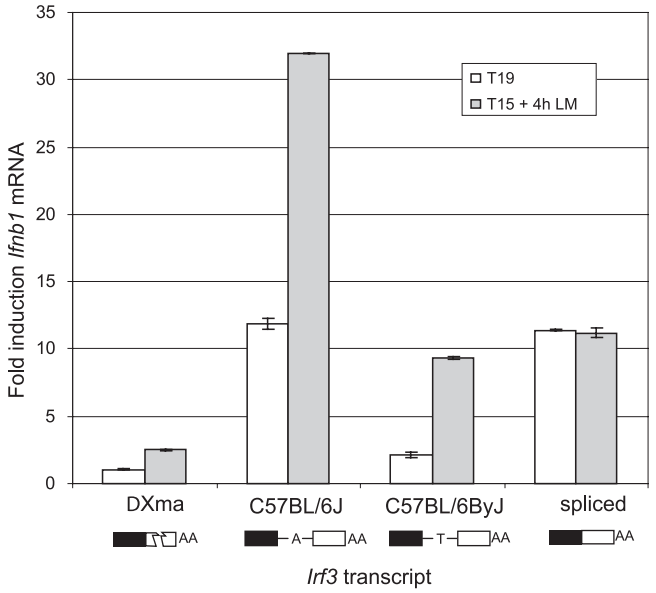

Figure 7. Levels of *Ifnb1* mRNA Expression in C57BL/6ByJ BMMs following Transfection of *Irf3* mRNAs That Are Fully Spliced, Contain Intron 5, or Deleted for IRF Domain (ΔXma)

Ifnb1 mRNA expression was measured by RT RT-PCR either 19 h (T19) following transfection or after 15 h transfection plus 4 h infection with *L. monocytogenes* (T15 + 4h LM). A representative of three independent experiments is shown.

doi:10.1371/journal.pgen.0030152.g007

[29,30] (Figure S4). Recent evidence indicates that splicing of U12-type introns could be a rate-limiting step in gene expression [31]. Our analysis suggests that this may also be the case for intron 5 in the murine *Irf3* gene. Macrophages from common strains, such as C57BL/6J and BALB/cByJ, have two populations of *Irf3* transcripts: a major, fully spliced species and a minor species that retains intron 5 (see Figure 4A). The presence of multiple Genbank (i.e., BC082274, BC003233; http://www.ncbi.nlm.nih.gov/Genbank/index.html) and EST entries of *Irf3* mRNAs that retain intron 5 further supports this hypothesis. Therefore, the rate of intron 5 splicing could control the amount of IRF3 available in the cell. Interestingly, it has been shown that activity of human IRF3 is also regulated at the level of splicing [32]. However, in contrast to rodent *Irf3*, regulation of human *IRF3* involves alternative intron 1 splice acceptor sites that can produce an active or a dominant negative, *IRF3a*, form of *IRF3* [33]. Because it appears that by converting to a U2 intron, human *IRF3* intron 5 lost its rate-limiting function, it is intriguing to contemplate that this led to emergence of an alternative splicing control mechanism for human *IRF3*.

Our choice of mouse strains for genetic analysis of susceptibility to *L. monocytogenes* infection was based on the existence of the ByJ-based CXB RI mapping panel. The C57BL/6By substrain has been used to generate at least seven of the 13 CXB RI strains, but none of the CXB strains appear to have a defect in induction of *Ifnb1*. To resolve this discrepancy, we sequenced *Irf3* intron 5 in all C57BL/6By-derived CXB strains. None of the sequenced *Irf3* introns contained the mutation found in the C57BL/6ByJ strain (unpublished data). Therefore, it appears that the A to T mutation rose in the C57BL/6ByJ background only recently, after the generation of the CXB RI strains. It is possible that the return of D. W. Bailey's substrains to the Production Department of Jackson Laboratories in 1974 could have created a bottleneck that fixed the mutation in the current C57BL/6ByJ population.

Splicing of mRNA is a critical step in protein expression, and in humans, genetic polymorphisms that produce aberrant or alternate splicing products have been associated with a wide range of diseases [34]. We used genetic analysis of the mouse model system to provide definitive evidence of the important role of splicing in control of infection. We found that a mouse substrain-specific defect in induction of *Ifnb1* is due to a single nucleotide polymorphism in intron 5 of *Irf3*. Our analysis of this polymorphism revealed that splicing is a critical step in the control of *Irf3* expression and, as a result, in the course and outcome of *L. monocytogenes* infection. While intron 5 of murine *Irf3* has features of both U2 and U12 introns, we provide evidence that its splicing is dependent on the U12 spliceosome. Therefore, it appears that in rodents the U12 spliceosome can use U2 splice sites. This suggests that the spectrum of U12-type introns present in mammalian genomes could be wider than previously thought. Finally, our comparison of rodent and primate *Irf3* genomic sequences also revealed the intriguing possibility that we have identified an intermediate step in the process of conversion from a U12- to U2-type intron.

Materials and Methods

Animals. Six-to-twelve-week-old animals were used in all experiments. BALB/cByJ, C57BL/6J, and C57BL/6ByJ mice were obtained from Jackson Laboratories (http://www.jax.org/). B/ByJ.C N2 mice were created by backcrossing B/ByJ.C F1 males to C57BL/6ByJ females. All mouse strains were bred and maintained under specific pathogen-free conditions in the animal facilities at the University of Massachussetts Medical School. All experiments involving live animals were carried out in accordance with the guidelines set forth by the University of Massachussetts Medical School Department of Animal Medicine and the Institute Animal Care and Use Committee.

In vivo infections. Pre-titered TSB-glycerol stocks of *L. moncytogenes* strain 10403S were stored at −80 °C. Prior to infection, 1-ml bacterial aliquots were recovered for 1 h at 37 °C in 9 ml of TSB (BD Biosciences, ttp://www.bdbiosciences.com/), washed, and resuspended to the desired cfu in PBS. Mice were injected with a defined dose of *L. monocytogenes* strain 10403S in 0.4 ml of PBS. At defined time points, infected animals were killed by CO_2 asphyxiation. Livers and spleens of infected animals were aseptically harvested, weighed, and homogenized in 0.02% Triton X-100. Aliquots of serial 5-fold dilutions in sterile water were plated in duplicate on TSB agar (BD Biosciences) plates containing 10 μg/ml streptomycin. After overnight incubation, the number of bacteria per milligram of tissue was determined by counting colonies at the appropriate dilution.

Generation of bone marrow macrophages. BMMs were generated by differentiating bone marrow calls in a complete BM medium (DMEM, 10% heat-inactivated FCS (Invitrogen, http://www.invitrogen.com/), 100 U/ml penicillin (Invitrogen), 100 μg/ml streptomycin (Invitrogen), and 10% L929 fibroblast-conditioned medium as a source of M-CSF) for 6 d in 10-cm Petri dishes (VWR, http://www.vwr.com/).

Cell lines. Fibroblast-like YF5 and macrophage-like YM14 cell lines were generated by immortalization of C57BL/6ByJ bone marrow cells as previously described [35,36]. Clones were selected based on morphology.

Ex vivo experiments. Differentiated BMMs were detached from the Petri plates by incubation in cold PBS, washed, resuspended in BM medium without antibiotics and used to seed multiwell dishes at 1×10^5 cells/cm^2. Following overnight incubation the medium was replaced with DMEM containing the agent used to stimulate BMM. For *L. monocytogenes*, after 1 h the medium was replaced with BM medium containing 10 μg/ml gentamicin (Fisher) to remove extracellular bacteria. Lipopolysaccharide (Sigma) was added at 1 μg/ml, poly I:poly C (Sigma) at 25 μg/ml and Sendai Virus (generous gift of Kate Fitzgerald, University of Massachussetts) at 200 U/ml. At defined

timepoins BMMs were lysed in TRIzol (Invitrogen) and RNA was isolated according to manufacturer's protocol.

BMM cell death assay. 5×10^4 BMMs were seeded in 96-well tissue culture plate and following overnight incubation the cells were infected with a defined multiplicity of infection (MOI) of *L. monocytogenes*. After 1 h incubation, the cell culture medium was replaced with medium containing 10 μg/ml of gentamicin (MP Biomedicals, http://www.mpbio.com/). At defined time points the supernatants were collected and the remaining cells were lysed for 20 min at room temperature in 50 μl/well of complete medium plus 1μl of cell lysis solution from CytoTox-ONE Homogeneous Membrane Integrity Assay kit (Promega, http://www.promega.com/). Lactose dehydrogenase (LDH) assay for supernatants and cell lysates was performed according to the manufacturer's protocol. Fluorescence was recorded at 560/590 nm using a Synergy HT microplate reader (Bio-Tek, http://www.biotek.com/). The relative concentration of LDH in supernatants was calculated by the equation: 100% × (LDHsup/(LDHsup+LDHcell)).

Real time PCR. Relative mRNA levels were quantified by real time RT-PCR on an ABI 7300 instrument (http://www.appliedbiosystems.com/) utilizing SYBR Green chemistry (ABI SYBR master mix + RT reagents). Generally, 50 ng of total RNA was used in 20 ml one-step reactions that incorporated a 30-min reverse transcription step prior to cycling. Primers used to detect specific mRNAs are described in Table S1. Ribosomal protein S17 *(Rps17)* and actin mRNA were used as a loading controls. To quantify the relative amounts of mRNA in each experiment, 2-fold dilutions were used to create calibration curves. Each experiment included at least two biological and three experimental replicates.

Genetic mapping. BMMs from 46 B/ByJ(C.B/ByJ) N2 mice were infected in duplicate with *L. monocytogenes* strain 10403S at MOI = 5. Four hours following infection, total RNA was isolated and used for real time RT-PCR analysis of *Ifnb1* mRNA induction. *Ifnb1* Ct values from duplicate samples were adjusted for variation in total RNA concentration using *Rps17* Ct values, transformed by subtracting the average C57BL/6ByJ parental value, and used directly as trait values for mapping using MapManger software. Under ideal conditions, such transformed Ct values can be viewed as $\log_2$ of the fold difference in *Ifnb1* expression compared to the C57BL/6ByJ parent. A genetic map was constructed using 56 microsatelite markers [16]. Experimental *p*-value for linkage was evaluated using a built-in permutation test and was found to be less than 10^{-4}.

IRF3 immunoblotting. BMMs were infected with *L. monocytogenes* (MOI = 5) or Sendai Virus (600 HU) for 4 h. Cells were lysed in the presence of protease inhibitors (Roche, http://www.roche.com/) and following centrifugation, supernatant aliquots containing 20 μg of protein were loaded per lane of a native polyacrylamide gel. IRF3 was detected by immunoblotting with an anti-IRF3 antibody (Invitrogen). For total IRF3 protein analysis, lysates were obtained from infected and uninfected BMMs treated with either 10 μM MG-132 proteasome inhibitor or DMSO vehicle. Three micrograms of total protein were separated on denaturing SDS polyacrylamide gel and immumoblotted with anti IRF-3 antibobody (Invitorgen).

RNA transfection. The cDNAs of fully spliced *Irf3, Irf3* lacking internal XmaI fragment, and strain-specific *Irf3* species retaining intron 5 were amplified with IRF3F+1 and IRF3dT32SspIR oligonucleotides (Table S1). IRF3dT32SspIR was designed to introduce poly(A)$_{32}$ and a unique SspI site at the 3′ end of *Irf3* coding sequences. Amplified *Irf3* fragments were cloned in front of T7 promoter of pCR2.1 vector (Invitrogen). To generate *Irf3* mRNAs, 1 μg of respective SspI linearized plasmids was used as templates in in vitro transcription reactions (Maxiscript T7; Ambion, http://www.ambion.com/). One microgram of DNAse treated, reprecipitated RNA was used for nucleofection of 1 to 1.5×10^6 BMMs in 100 μl of complete mouse macrophage nucleofector solution (82 μl mouse macrophage nucleofector solution plus 18 μl supplement) from Mouse Macrophage Nucleofector kit (Amaxa Biosystems, http://www.amaxa.com/). Following electroporation using a Nucleofector II electroporation device (Amaxa) with program Y-001, cells were split into two wells of a 24-well culture plate, each containing 1 ml of RPMI/10% FBS/10% LCCM medium.

Flow cytometry. Splenocytes were isolated by disrupting aseptically harvested spleens in RPMI 10% FCS using a 70-μm pore size mesh cell strainer (BD Biosciences) to obtain single-cell suspensions. Red blood cells were lysed in ACK buffer (Sigma-Aldrich, http://www.sigmaaldrich.com/). Splenocytes were resuspended to obtain 2×10^7 cells/ml in HBSS supplemented with 0.5% and 0.1% NaN_3. Each sample containing 1×10^6 cells was blocked with FcR-blocking antibody (CD16/CD32) and stained with respective directly conjugated antibodies and their isotype controls. Stained cells were fixed in 1% paraformaldehyde (Sigma-Aldrich) for 24 h prior to analysis using a FACScan flow cytometer (BD Biosciences).

Splicing assays. C57BL/6J and C57BL/6ByJ minigene constructs were generated by cloning *Irf3* intron 5 flanked by 250 bp of exonic sequences into the vector pcDNA3 (Invitrogen), to create pINT5J and pINT5ByJ, respectively. For ex vivo splicing assays, the C57BL/6ByJ-derived fibroblast-like cell line Y5 was transfected with either pINT5J or pINT5ByJ, and splicing was monitored 12 h later by real time RT-PCR using primers specific to the transcribed vector sequence (pCDNA3F3) and either intron 5 (IRF3IntR) or the exon 5–6 junction (IRF3Ex5/6R5,). For in vitro splicing assays, minigene *Irf3* pre-mRNA templates were PCR-amplified from pINT5J and pINT5ByJ using a T7-containing primer, purified, and transcribed in vitro using T7 polymerase in the presence of [alpha-^{32}P]UTP. In vitro splicing reactions were performed essentially as described previously [37], except that 30% HeLa nuclear extract was used. Spliced products were resolved on 12% denaturing polyacrylamide gels (19:1) in 8 M urea in Tris-Borate-EDTA buffer, and visualized using a Fujifilm FLA-500 phosphorimager (http://www.fujifilm.com/). U2 and U12 snRNAs were inactivated by RNase H–directed cleavage as described previously [38] using DNA oligonucleotides complementary to nucleotides 27–49 of the U2 snRNA or to nucleotides 11–28 of the U12 snRNA.

Genes. All genes mentioned in the text and their corresponding National Center for Biotechnology Information (NCBI) GeneID (http://www.ncbi.nlm.nih.gov/sites/gquery) and Ensembl (http://www.ensembl.org/) identifiers are described in Table S2.

Supporting Information

Figure S1. Levels of *Ifnb1* mRNA in Tissues of Infected Animals

Ifnb1 mRNA was not detectable in livers and spleens of animals infected with 1×10^5 *L. monocytogenes* until the 24-h time point. Forty-eight hours after infection, spleens of C57BL/6J animals had 6-fold higher levels of *Ifnb1* mRNA than C57BL/6ByJ animals.

Found at doi:10.1371/journal.pgen.0030152.sg001 (238 KB EPS).

Figure S2. Survival of C57BL/6J and C57BL/6ByJ Mice following Intravenous Infection with 1×10^5 cfu *L. monocytogenes* Strain 10403S

The majority of C57BL/6ByJ mice survive for more then 10 d following infection.

Found at doi:10.1371/journal.pgen.0030152.sg002 (72 KB EPS).

Figure S3. MapManager QTX Chromosome 7 Interval Mapping Results

Likelihood ratio statistic scores represent thresholds of suggestive, significant, and highly significant linkages, respectively.

Found at doi:10.1371/journal.pgen.0030152.sg003 (206 KB EPS).

Figure S4. High Levels of Spliced *Irf3* mRNA Induce Death of BMMs

Survival of C57BL/6J *Irf3*$^{-/-}$ BMMs following 24-h transfection of in vitro transcribed *Irf3* mRNAs was monitored by the release of the cytosolic enzyme LDH into the supernatant.

Found at doi:10.1371/journal.pgen.0030152.sg004 (240 KB EPS).

Table S1. Sequences of Primers Used in This Study

Found at doi:10.1371/journal.pgen.0030152.st001 (19 KB PDF).

Table S2. NCBI GeneID and Ensembl Identifiers for Genes Mentioned in the Text

Found at doi:10.1371/journal.pgen.0030152.st002 (27 KB PDF).

Acknowledgments

We thank Kate Fitzgerald for providing reagents for this study, Paul Kaufman, Ingolf Bach, Brian Lewis, Ashild Vik, and Sara Evans for helpful discussion and critical reading of the manuscript.

Author contributions. MRG and VB conceived and designed the experiments. OG, ZQ, HS, and SP performed the experiments. OG, ZQ, HS, MRG, and VB analyzed the data. VB wrote the paper.

Funding. This work was supported by the National Institute of Allergy and Infectious Diseases grant AI060991 to VB.

Competing interests. The authors have declared that no competing interests exist.

References

1. Stetson DB, Medzhitov R (2006) Recognition of cytosolic DNA activates an IRF3-dependent innate immune response. Immunity 24: 93–103.
2. Stockinger S, Reutterer B, Schaljo B, Schellack C, Brunner S, et al. (2004) IFN regulatory factor 3-dependent induction of type I IFNs by intracellular bacteria is mediated by a TLR- and Nod2-independent mechanism. J Immunol 173: 7416–7425.
3. Stockinger S, Materna T, Stoiber D, Bayr L, Steinborn R, et al. (2002) Production of type I IFN sensitizes macrophages to cell death induced by *Listeria monocytogenes*. J Immunol 169: 6522–6529.
4. O'Connell RM, Saha SK, Vaidya SA, Bruhn KW, Miranda GA, et al. (2004) Type I interferon production enhances susceptibility to *Listeria monocytogenes* infection. J Exp Med 200: 437–445.
5. Auerbuch V, Brockstedt DG, Meyer-Morse N, O'Riordan M, Portnoy DA (2004) Mice lacking the type I interferon receptor are resistant to *Listeria monocytogenes*. J Exp Med 200: 527–533.
6. Carrero JA, Calderon B, Unanue ER (2004) Type I interferon sensitizes lymphocytes to apoptosis and reduces resistance to *Listeria* infection. J Exp Med 200: 535–540.
7. O'Connell RM, Vaidya SA, Perry AK, Saha SK, Dempsey PW, et al. (2005) Immune activation of type I IFNs by *Listeria monocytogenes* occurs independently of TLR4, TLR2, and receptor interacting protein 2 but involves TNFR-associated NF kappa B kinase-binding kinase 1. J Immunol 174: 1602–1607.
8. Carrero JA, Calderon B, Unanue ER (2006) Lymphocytes are detrimental during the early innate immune response against *Listeria monocytogenes*. J Exp Med 203: 933–940.
9. Zheng SJ, Jiang J, Shen H, Chen YH (2004) Reduced apoptosis and ameliorated listeriosis in TRAIL-null mice. J Immunol 173: 5652–5658.
10. Garifulin O, Boyartchuk V (2005) *Listeria monocytogenes* as a probe of immune function. Brief Funct Genomic Proteomic 4: 258–269.
11. Boyartchuk VL, Broman KW, Mosher RE, D'Orazio SE, Starnbach MN, et al. (2001) Multigenic control of *Listeria monocytogenes* susceptibility in mice. Nat Genet 27: 259–260.
12. Dux A, Muhlbock O, Bailey DW (1978) Genetic analyses of differences in incidence of mammary tumors and reticulum cell neoplasms with the use of recombinant inbred lines of mice. J Natl Cancer Inst 61: 1125–1129.
13. Mahieu T, Park JM, Revets H, Pasche B, Lengeling A, et al. (2006) The wild-derived inbred mouse strain SPRET/Ei is resistant to LPS and defective in IFN-beta production. Proc Natl Acad Sci U S A 103: 2292–2297.
14. Perry AK, Chen G, Zheng D, Tang H, Cheng G (2005) The host type I interferon response to viral and bacterial infections. Cell Res 15: 407–422.
15. Seth RB, Sun L, Ea CK, Chen ZJ (2005) Identification and characterization of MAVS, a mitochondrial antiviral signaling protein that activates NF-kappaB and IRF 3. Cell 122: 669–682.
16. Dietrich WF, Miller JC, Steen RG, Merchant M, Damron D, et al. (1994) A genetic map of the mouse with 4,006 simple sequence length polymorphisms. Nat Genet 7: 220–245.
17. Manly KF, Cudmore RH Jr., Meer JM (2001) Map Manager QTX, cross-platform software for genetic mapping. Mamm Genome 12: 930–932.
18. Manichaikul A, Dupuis J, Sen S, Broman KW (2006) Poor performance of bootstrap confidence intervals for the location of a quantitative trait locus. Genetics 174: 481–489.
19. Sato M, Suemori H, Hata N, Asagiri M, Ogasawara K, et al. (2000) Distinct and essential roles of transcription factors IRF-3 and IRF-7 in response to viruses for IFN-alpha/beta gene induction. Immunity 13: 539–548.
20. Honda K, Yanai H, Negishi H, Asagiri M, Sato M, et al. (2005) IRF-7 is the master regulator of type-I interferon-dependent immune responses. Nature 434: 772–777.
21. Hwang DY, Cohen JB (1997) A splicing enhancer in the 3′-terminal c-H-ras exon influences mRNA abundance and transforming activity. J Virol 71: 6416–6426.
22. Jurica MS, Moore MJ (2003) Pre-mRNA splicing: Awash in a sea of proteins. Mol Cell 12: 5–14.
23. Jackson IJ (1991) A reappraisal of non-consensus mRNA splice sites. Nucleic Acids Res 19: 3795–3798.
24. Hall SL, Padgett RA (1994) Conserved sequences in a class of rare eukaryotic nuclear introns with non-consensus splice sites. J Mol Biol 239: 357–365.
25. Burge CB, Padgett RA, Sharp PA (1998) Evolutionary fates and origins of U12-type introns. Mol Cell 2: 773–785.
26. Kim DH, Longo M, Han Y, Lundberg P, Cantin E, et al. (2004) Interferon induction by siRNAs and ssRNAs synthesized by phage polymerase. Nat Biotechnol 22: 321–325.
27. Pichlmair A, Schulz O, Tan CP, Naslund TI, Liljestrom P, et al. (2006) RIG-I-mediated antiviral responses to single-stranded RNA bearing 5′-phosphates. Science 314: 997–1001.
28. Hornung V, Ellegast J, Kim S, Brzozka K, Jung A, et al. (2006) 5′-Triphosphate RNA is the ligand for RIG-I. Science 314: 994–997.
29. Heylbroeck C, Balachandran S, Servant MJ, DeLuca C, Barber GN, et al. (2000) The IRF-3 transcription factor mediates Sendai virus-induced apoptosis. J Virol 74: 3781–3792.
30. Kim TK, Lee JS, Jung JE, Oh SY, Kwak S, et al. (2006) Interferon regulatory factor 3 activates p53-dependent cell growth inhibition. Cancer Lett 242: 215–221.
31. Patel AA, McCarthy M, Steitz JA (2002) The splicing of U12-type introns can be a rate-limiting step in gene expression. EMBO J 21: 3804–3815.
32. Karpova AY, Howley PM, Ronco LV (2000) Dual utilization of an acceptor/donor splice site governs the alternative splicing of the IRF-3 gene. Genes Dev 14: 2813–2818.
33. Karpova AY, Ronco LV, Howley PM (2001) Functional characterization of interferon regulatory factor 3a (IRF-3a), an alternative splice isoform of IRF-3. Mol Cell Biol 21: 4169–4176.
34. Nissim-Rafinia M, Kerem B (2002) Splicing regulation as a potential genetic modifier. Trends Genet 18: 123–127.
35. Ogawa Y, Ohno N, Ito M, Iizuka M, Kobayashi S, et al. (1991) Generation of functional murine macrophage lines employing a helper-free and replication-defective SV40-retrovirus: Cytokine-dependent growth. Cell Struct Funct 16: 467–474.
36. Kreuzburg-Duffy UC, MacDonald C (1994) Establishment and characterization of murine macrophage-like cell lines following transformation with simian virus 40 DNA deleted at the origin of replication. J Immunol Methods 174: 33–51.
37. Kan JL, Green MR (1999) Pre-mRNA splicing of IgM exons M1 and M2 is directed by a juxtaposed splicing enhancer and inhibitor. Genes Dev 13: 462–471.
38. Merendino L, Guth S, Bilbao D, Martinez C, Valcarcel J (1999) Inhibition of msl-2 splicing by Sex-lethal reveals interaction between U2AF35 and the 3′ splice site AG. Nature 402: 838–841.